SCIENTIFIC REPORTS

OPEN

SUBJECT AREAS:
ENVIRONMENTAL MONITORING
IR SPECTROSCOPY

Received
1 April 2014

Accepted
3 June 2014

Published
9 July 2014

Correspondence and requests for materials should be addressed to X.L. (xyli@dlut.edu.cn) or J.C. (jhchen@uwm.edu)

Ultrasensitive Quantum Dot Fluorescence quenching Assay for Selective Detection of Mercury Ions in Drinking Water

Jun Ke[1], Xinyong Li[1], Qidong Zhao[1], Yang Hou[2] & Junhong Chen[2]

[1]State Key Laboratory of Fine Chemicals, Key Laboratory of Industrial Ecology and Environmental Engineering (MOE), School of Environmental Science and Technology, Dalian University of Technology, Dalian, 116024, China, [2]Department of Mechanical Engineering, University of Wisconsin-Milwaukee, Milwaukee, WI 53211, USA.

Mercury is one of the most acutely toxic substances at trace level to human health and living thing. Developing a rapid, cheap and water soluble metal sensor for detecting mercury ions at ppb level remains a challenge. Herein, a metal sensor consisting of MPA coated Mn doped ZnSe/ZnS colloidal nanoparticles was utilized to ultrasensitively and selectively detect Hg^{2+} ions with a low detection limit (0.1 nM) over a dynamic range from 0 to 20 nM. According to strong interaction between thiol(s) and mercury ions, mercaptopropionic acid (MPA) was used as a highly unique acceptor for mercury ions in the as-obtained ultrasensitive sensor. In the presence of mercury ions, colloidal nanoparticles rapidly agglomerated due to changes of surface chemical properties, which results in severe quenching of fluorescent intensity. Meanwhile, we find that the original ligands are separated from the surface of colloidal nanoparticles involving strongly chelation between mercury ion and thiol(s) proved by controlled IR analysis. The result shows that the QD-based metal ions sensor possesses satisfactory precision, high sensitivity and selectivity, and could be applied for the quantification analysis of real samples.

Heavy metal ions, particularly mercury ions, are detrimental to human health due to their high toxicity, mobility, and ability to accumulate through food chains or atmosphere in the ecological system[1–3]. Cell toxicity of mercury has been intensively studied by environmental and biological communities over the years. Its low concentration but high toxicity makes mercury contamination a global environmental problem[4–6]. Therefore, ultrasensitive determination of mercury is essential to provide evaluation index of mercury ions in aqueous environment. However, compared with analysis methods based on sophisticated and time-consuming instruments[7–8], developing facile and efficient methods for rapid quantitative analysis of mercury ions in real samples remains a challenge.

In the past decade, the field of biological and chemical nanosensors that utilize fluorescent semiconducting materials has witnessed an explosion because of unique optical properties of fluorescent semiconducting materials[9–13]. Fluorescent probes based on semiconducting colloidal nanoparticles, such as quantum dots (QDs), have received growing attention because of their unique size-dependent optical properties[14–16]. These fluorescent colloidal nanoparticles dispersed stably in an aqueous solution are often encapsulated and protected by thiol functional group[17–20]. Previous studies have reported that metal ions could interact with colloidal nanoparticles or fluorescent dyes by coordinate bond such as metal-sulfide bond, which consequently results in drastic fluctuation and quenching of fluorescent intensity due to electron transfer even aggregation of colloidal nanoparticles[21–24]. In light of such signal fluctuation, a series of effective approaches could be used to detect heavy metal ions and to investigate interactions between colloidal nanoparticles and heavy metal ions.

In this work, we take advantage of functionalized Mn-doped ZnSe/ZnS quantum dots to selectively and rapidly detect Hg^{2+} ions in real drinking water. Stable and water-soluble Mn-doped ZnSe/ZnS colloidal nanoparticles with bright yellow emission were successfully prepared through nucleation doping followed by shell epitaxial growth and successive ion layer adsorption and reaction (SILAR). The emission of the fluorescent probe solution is quenched following the addition of mercury ions with a short response time (<30 s), which is suitable for in-situ chemosensors. The possible interaction between colloidal nanoparticles and mercury ions was proposed and proved by using FT-IR spectroscopy, which revealed changes of surface properties when mercury ions were added.

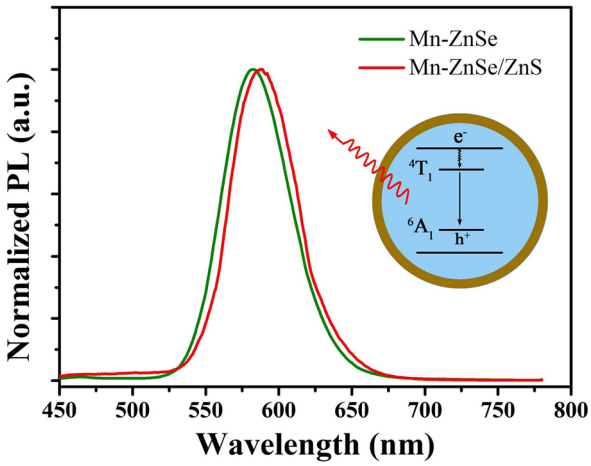

Figure 1 | Photoluminescence spectra of Mn-doped ZnSe QDs and Mn-doped ZnSe/ZnS QDs. The excitation wavelength was 420 nm.

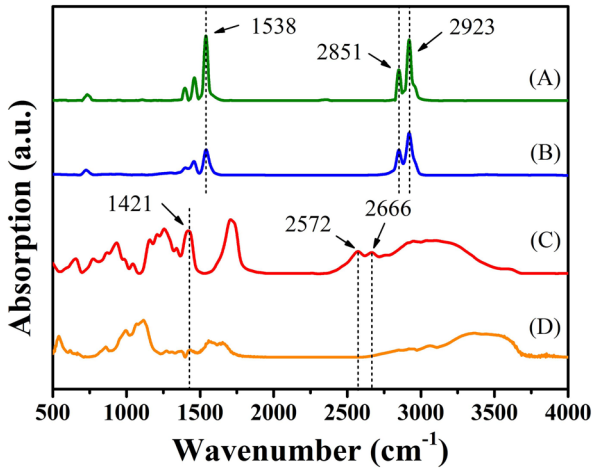

Figure 2 | FTIR spectra of the samples before and after the ligand exchange. (A) pure Zn stearate, (B) stearate acid-coated QDs, (C) pure MPA, (D) MPA-coated QDs.

Results and Discussion

Preparation of Highly Emissive Colloidal Nanoparticles. Quantum dots could emit fluorescence upon excited by using different wavelengths of light. The intensity of fluorescent signal can be used to indicate the change in the surface microenvironment of colloidal nanoparticles, such as a pH value indicator. To obtain highly emissive colloidal nanoparticles, we firstly prepared Mn-doped ZnSe QDs through a general synthesis route called "nucleation-doping" without using highly toxic organo-phosphines[25,26]. The Mn-doped ZnSe QDs possessed highly emissive dopant photoluminescence (PL) centred at about 584 nm which is attributed to the $^4T_1 \rightarrow {}^6A_1$ transition for Mn^{2+} ions in the ZnSe lattice (Figure 1)[27–30].

To reduce surface traps and lower the non-radioactive transition, the introduction of a wide band-gap ZnS shell is necessary[31,32]. Before epitaxial growth of an inorganic shell on the core in the aqueous solution, hydrophobic colloidal nanoparticles coated with stearate acid were transferred into water, which makes it convenient for further utilizing colloidal QDs. Mercaptopropionic acid (MPA) was used as a hydrophilic ligand to replace the hydrophobic ligand attached to the surface of the as-synthesized QDs. The replacement of surface ligands successfully occurred, which was confirmed through phase transfer phenomenon (see Supporting Information, Figure S1). After the formation of a ZnS shell, we observed that the fluorescent intensity was apparently enhanced, which suggests that charge carriers are well confined within the core region and separated from the surface because of the well-defined epitaxial ZnS shell on the surface of the ZnSe core[31]. The quantum yield (QY) of Mn-doped ZnSe/ZnS core/shell QDs was improved to 25%, greater than that of bare Mn-doped ZnSe (5%). Meanwhile, the peak of PL shifted from 584 nm to 588 nm, which is attributed to the enhancement of crystal field of isolated Mn ions in the lattice of ZnSe with the growth of the ZnS shell[33]. The ratio of thiol to QDs was measured, up to 1870 : 1, which ensured the water soluble QDs could be stable and emissive in aqueous solution.

FT-IR spectra demonstrated successful ligand change from hydrophobic SA to hydrophilic MPA (Figure 2). The vibration peak at 1538 cm^{-1} attributed to C = O stretching demonstrates that the as-prepared colloidal nanoparticles were encapsulated by original stearate ligands. These characteristic peaks of stearate at 2851 cm^{-1} and 2923 cm^{-1} attributed to C-H symmetric vibration almost disappeared after the ligand exchange. The vibration peak at 1421 cm^{-1} due to S-CH_2 wagging vibration and the absence of the S-H stretching bond between 2666 cm^{-1} and 2572 cm^{-1} suggest the attachment of MPA molecule to QDs through chemical bond between thiols and dangling Zn atoms of the ZnSe layer[32]. Compared with the IR spectrum of pure MPA (liquid film), stretching vibration peak of C = O at 1712 cm^{-1} shifts to a lower wavenumber due to spatial distortion resulting from the high density ligand layer.

The formation of a ZnS shell around the ZnSe core has been confirmed by transmission electron microscopy (TEM). A typical TEM image (Figure 3a) shows that the average diameter of Mn-doped ZnSe/ZnS core/shell colloidal nanoparticles is about 6.0 nm. The hydrodynamic diameters (Figure 4) were further determined by dynamic light scattering (DLS). In agreement with TEM results, the hydrodynamic diameters of as-obtained colloidal nanoparticles are 6.5 nm, which indicates that the dispersed QDs turned out to be individual monomeric state. The larger diameter in the DLS data is due to the outmost hydration layer which increases the diameter of colloidal nanoparticles[34].

Influence of pH Values on the Stability of Colloidal Nanoparticles in an Aqueous Solution. To understand effects of aquatic condition on the as-prepared fluorescent colloidal nanoparticles, we investigated the stability of MPA-coated Mn-doped ZnSe/ZnS colloidal nanoparticles under different pH conditions. The stability of colloidal nanoparticles in water depends on the interaction balance between van der Waals attractive forces and electrostatic repulsive forces among these colloidal nanoparticles according to Derjagui-Landau and Verwey-Overbeek theory (D.L.V.O theory)[35,36]. The surface potential of colloidal nanoparticles could to some extent influence the stability of colloidal nanoparticles[37,38]. To confirm the correlation, we added the water-soluble samples into solution with different pH values to tune the surface potential of colloidal nanoparticles[39,40]. We observed that the fluorescent intensity of samples increased with the increase of pH values (Figure 5). In the meantime, the trend of changes in QY is similar to that of emission intensity (the inset in Figure 5). These results show that pH values could influence physical and chemical properties of colloidal nanoparticles. When pH values changed from 11 to 7, the dissociation reaction of thiol function groups played a key role in the surface potential of colloidal nanoparticles. When pH value of the solution was lowered to 5.0, the deprotonized thiol and carboxylate were protonized and the resulting ligands were separated from the surface of colloidal nanoparticles due to the dissociation reaction in the solution according to our previous studies[32]. As a result, surface traps were exposed, which reduces the possibility of irradiative recombination.

Ultrasensitive Detection of Hg^{2+} Ions. Upon the addition of Hg^{2+} ions into water-soluble colloidal nanoparticles, apparent changes in

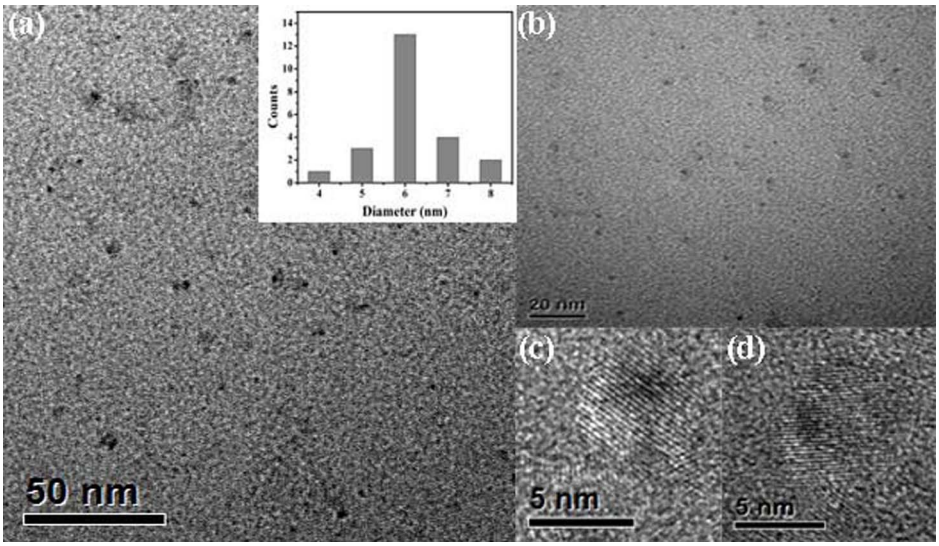

Figure 3 | **TEM (a, b) and HRTEM (c, d) images of MPA-coated Mn-ZnSe/ZnS QDs.**

the photoluminescence spectra can be observed from Figure 6a, which shows the fluorescence intensity of MPA-coated colloidal nanoparticles in the presence of Hg^{2+} ions (0–20 nM) in the phosphate buffered saline (PBS, 10 mM, 7.4) buffer solution. The emission intensity of colloidal nanoparticles was quenched obviously with the addition of Hg^{2+}. Meanwhile, the clear solution rapidly became turbid due to the aggregation of colloidal nanoparticles. In general, ligands with thiol functional groups usually act as a useful protection layer to prevent colloidal nanoparticles from aggregating during synthesis and storage. However, we found that the characteristic peaks of ligands disappeared, such as C-S bond at 1419 cm^{-1} and C = O bond at 1546 cm^{-1}, after the addition of mercury ions (Figure 7). The aggregation of colloidal nanoparticles is, therefore, attributed to the separation of the organic passivation layer from the surface of colloidal nanoparticles in the presence of Hg^{2+} ions (Figure 8). The emission signal response to mercury ions could thus be utilized to detect mercury ions in aqueous solution. For the as-fabricated chemosensor, the limit of detection (LOD) is 0.1 nM which is lower than those of chemosensors based on QDs reported in our previous study and by other research groups[21,32,41]. Compared with our previous study, Mn dopant in this work enhances the emission intensity of QDs and acts as a signal donor, which is beneficial for amplifying the effect of mercury ions, thereby improving the sensitivity and lowering the limit of detection.

Selectivity for Mercury Ions. In order to investigate the selective interaction between colloidal nanoparticles and Hg^{2+} which is necessary for practical applications, the luminescence features of colloidal nanoparticles were measured in the presence of nine heavy metal ions other than Hg^{2+}, including Co^{2+}, Cd^{2+}, Ag^{+}, Pb^{2+}, Fe^{3+}, Cr^{3+}, Cu^{2+}, Zn^{2+}, and Ni^{2+}. MPA-coated Mn-doped ZnSe/ZnS colloidal nanoparticles did not show significant responses to these metal ions (Figure 9). This result suggests that compared with Hg^{2+} ions these heavy metal ions only slightly quenched the photoluminescence intensity of colloidal nanoparticles due to the weak affinity between these heavy metal ions and the thiol. The relative bond strength of metal-sulfides is determined by their respective K_{sp} value[42,43]. The slight quenching of emission by adding other heavy metal ions shows that the fluorescence of QDs also partially or completely quenched due to adsorption of heavy metal ions to the surface of QDs when high concentration of other heavy metal ions were added into thiol-coated QDs[44]. To further test the selectivity of probe solution, the fluorescence emission of MPA-coated Mn-doped ZnSe/ZnS colloidal nanoparticles could still be completely quenched by adding Hg^{2+} ions into probe solutions in the presence of other heavy metal ions (Supporting Information Figure S2), which indicates that other heavy metal ions have small influence on the interaction between mercury ions and surface thiol ligands within the range of measurements. Furthermore, these infrared characteristic peaks of ligands did not disappear even though other heavy metal ions were excessively added into the probe solution (Supporting Information Figure S3).

Detection of Real Samples. In order to identify the performance of the above chemosensor, we attempted to detect the concentration of mercury ions in drinking water samples. The sample collected was first filtered through a 0.22 μm membrane, then centrifuged for 5 min at 10000 rpm and detected according to the general

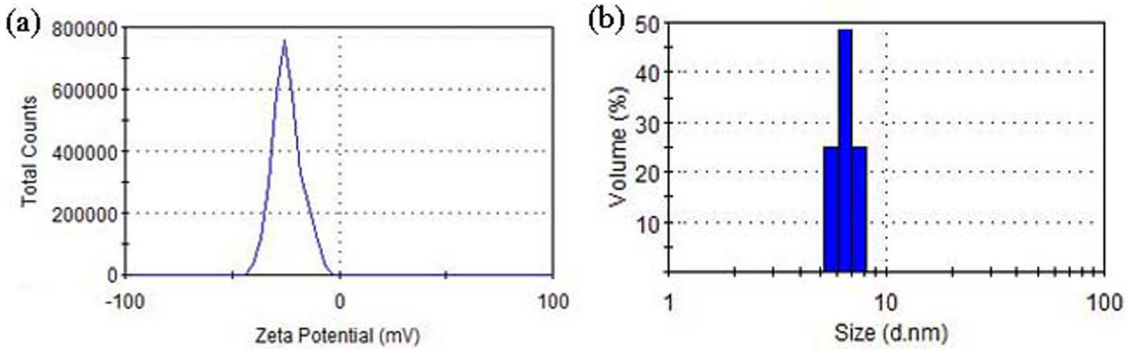

Figure 4 | **Hydrodynamic diameter of MPA-coated Mn-ZnSe/ZnS QDs measured by dynamic light scattering.**

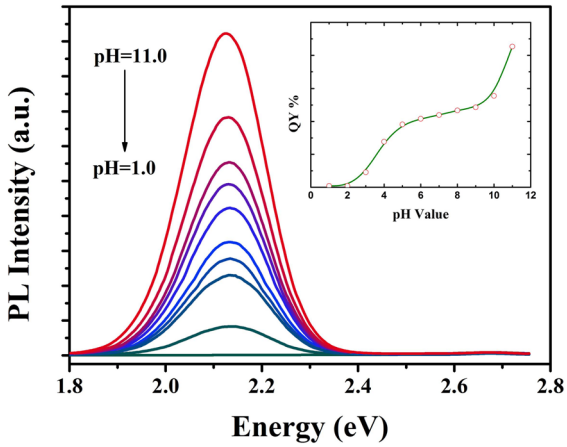

Figure 5 | Fluorescent spectra of MPA-coated Mn-ZnSe/ZnS QDs under different pH values. The inset: a correlation between QY of the samples vs. pH values.

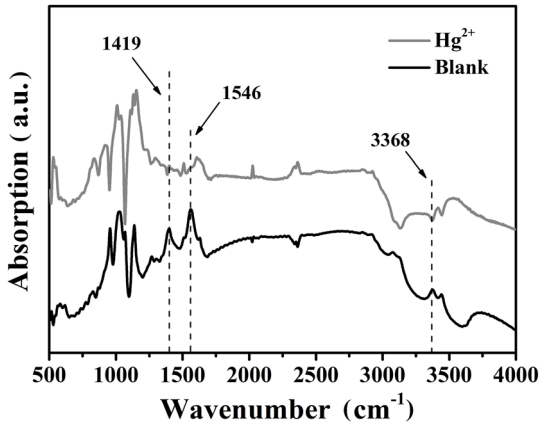

Figure 7 | FT-IR spectra of MPA-coated Mn-ZnSe/ZnS QDs in the presence of mercury ions (1 μM).

procedure with three successive runs. Based on the data obtained using the above procedure, the linear range of 0 nM to 1.5 nM was fitted into the equation of $I/I_0 = 0.969 - 1.555 \times C$, where C is the concentration of mercury ions in samples (Figure 6b). The experimental data resulting from the average of the three runs are displayed in Figure 10. The probe solution shows a high selectivity to mercury ions against a background of competing analytes, which displays a good applicability in real samples.

In conclusion, we have successfully fabricated Mn-doped ZnSe/ZnS colloidal nanoparticles through a nucleation doping process followed with SILAR. The resulting colloidal nanoparticles were applied to detect mercury ions up to 0.1 nM in drinking water. The doping of Mn not only increases the emission intensity of quantum dots, but also improves the sensitivity of the chemosensor. The strong bonding between thiol(s) and Hg^{2+} ions was critical for selective detection of mercury ions through IR analysis, which confirms the presence of thiol ligands and thus explains the aggregation of QDs.

Methods

Materials. Selenium powder (Se), mercaptopropionic acid (MPA), and n-dodicanethiol (DDT) were purchased from Acros Organics. 1-octadecene (ODE, 90%), oleylamine (OAm, 98%) was purchased from Tokyo Chemical Industry Co., LTD. Stearate acid (SA), Sodium stearate (NaSt) and Zinc stearate ($ZnSt_2$) were purchased from Sinopharm Chemical Reagent (Shanghai, China). All other reagents were of analytical grade and used without further treatment.

Synthesis of Manganese Stearate ($MnSt_2$). In a typical synthesis, NaSt (20 mmol) was dissolved in 80 g of methanol and heated to 50–60°C for 2 h until it became a clear solution and was then allowed to cool to room temperature. The solution of $MnCl_2$ was prepared by taking 10 mmol of $MnCl_2$ in 10 mL of methanol and mixed with the NaSt solution under vigorous stirring for 2 h. A white precipitation of $MnSt_2$ slowly flocculated. The obtained precipitations were repeatedly washed with methanol and dried under vacuum at 50°C.

Synthesis of Mn precursor and Zn precursor. The manganese precursor solution was prepared by mixing ODE (2.0 mL) with $MnSt_2$ (0.0414 g) and heated at 100°C until a formation of transparent solution. The zinc precursor solution was fabricated through adding ODE (5.0 mL) into the mixture of $Zn(St)_2$ (1.2008 g) and HSt (0.1081 g), and then temperature was raised to 150°C until solid reagent was completely dissolved under an inert atmosphere.

Preparation and Characterization of Colloidal Nanoparticles. Selenium powder (0.0790 g) and oleylamine (200 μL) in 20 mL ODE were added into a 50 mL three-neck flask and degassed at 120°C for 15 min by bubbling with nitrogen. The temperature of the mixture was then increased to 280°C and kept at the same temperature until selenium powder was completely dissolved. The manganese precursor solution (1 mL) was injected into the reaction flask at 280°C. And the reaction mixture was rapidly cooled to 260°C, lasting for 4 min to form MnSe nanoclusters. After the reaction temperature was lowered to 240°C, $ZnSt_2$ stock solution in ODE (0.5 mL) was injected into the reaction mixture for the formation of a ZnSe shell. 0.25 mL of oleylamine was added into the reaction solution to activate the zinc carboxylate. After growth for 50 min, the second and third $ZnSt_2$ stock solution (0.5 mL, respectively) were injected, each of which was followed by the same amount of oleylamine. The growth process of Mn-doped ZnSe QDs was monitored through UV-vis and PL measurement by taking aliquot samples. Finally, the reaction

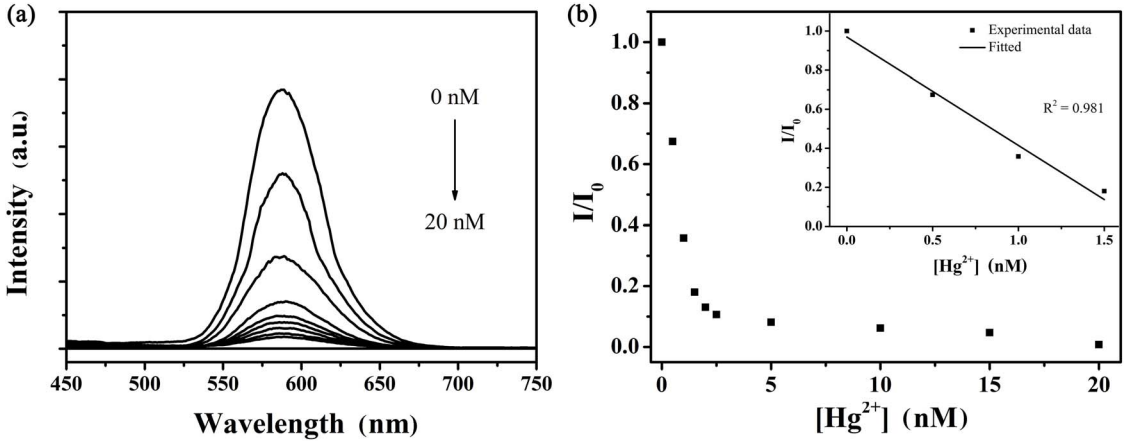

Figure 6 | (a) Photoluminescence spectra of MPA-coated Mn-ZnSe/ZnS QDs in PBS buffer (pH = 7.4) in the presence of different amounts of Hg^{2+} ions (0–20 nM). The excitation wavelength was 400 nm. (b) Calibration curve of the QD fluorescence at 588 nm *vs.* $[Hg^{2+}]$ (0–1.5 nM). The inset: a linear relationship between I/I_0 at 588 nm *vs.* $[Hg^{2+}]$ (0–1.5 nM), $R^2 = 0.981$.

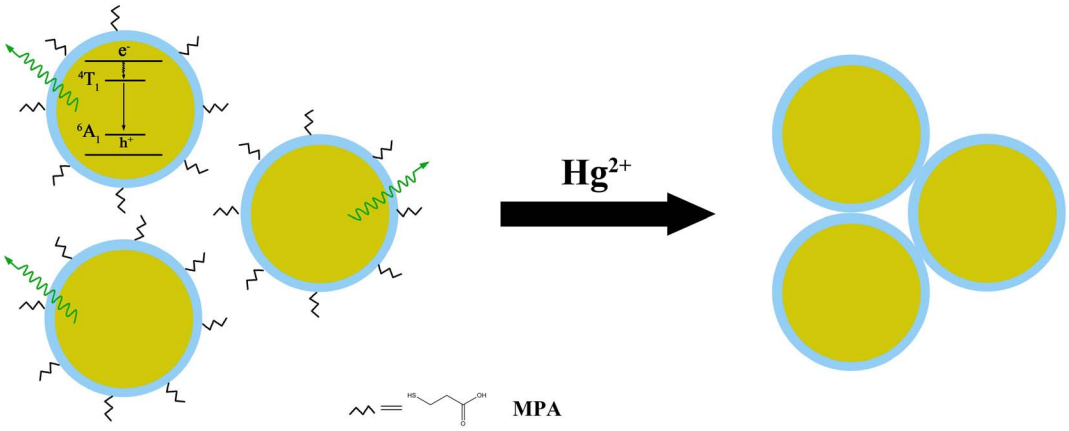

Figure 8 | The proposed sensing mechanism for Hg^{2+} ions based on metal-induced aggregation of QDs.

was allowed to cool down to room temperature, and the nanocrystals were purified by using a methanol/hexanes extraction process.

Prior to the growth of the ZnS shell, the core transferred into the aqueous solution by ligand exchange. A part of the as-obtained Mn-doped ZnSe QDs was redispersed into 2 mL chloroform solution. And 500 μL of MPA was added into the above solution, which was sonicated for 30 min to completely finish the exchange process. The precipitation was centrifuged, washed for at least three times using chloroform, and re-dispersed into a PBS solution. Highly luminescent, water soluble Mn-doped ZnSe/ZnS core/shell QDs were prepared through the successive ion layer adsorption and reaction (SILAR)[45]. The as-prepared water soluble MPA-capped Mn-ZnSe colloidal solution was diluted to 30 mL using deionized water in three-neck flask. And then a 10 mL of fresh aqueous solution containing zinc acetate and MPA was added into the colloidal solution under N_2 flow by stirring at room temperature. The pH value of the solution was adjusted to 11.0 using 2 M NaOH solution. The amount of zinc acetate and MPA (the molar ratio of Zn/MPA = 1 : 5) determines the desirable shell thickness of ZnS and the volume of the ZnSe core. The volume ratio between the core and the shell can be obtained using bulk lattice parameters of zinc blende ZnS. After 30 min stirring, The Na_2S aqueous solution was added into the solution (molar ratio of Zn/S = 1 : 1) at a step of 1 mL/min. The mixture was refluxed at 100°C for 2 h under stirring, and then Mn-doped ZnSe/ZnS core/shell QDs were obtained. The reaction was terminated by cooling the reaction mixture down to room temperature. The obtained MPA-capped Mn-doped ZnSe/ZnS core/shell QDs was purified *via* the standard two-step centrifugation process with the addition of acetone and ethanol to remove unreacted precursors. The as-obtained Mn-doped ZnSe/ZnS core/shell QDs were dispersed in the PBS buffer solution.

The UV-vis absorption spectra were taken on a spectrometer from Shanghai Tianmei Tech Ltd UV1100. The room temperature PL spectra of the QD samples were measured using a Hitch F-4500 fluorescence spectrometer. The PL quantum yield (QY) for Mn-doped ZnSe/ZnS QDs were calculated through referencing to a standard (RhB 6G in ethanol, QY = 95%, emission range: 500–700 nm) using the following equation[32].

$$\phi = \phi' \times \left(\frac{I}{I'}\right) \times \left(\frac{A'}{A}\right) \times \left(\frac{n}{n'}\right)^2$$

where ϕ and ϕ' are the PL QY for the QD sample and organic dye, respectively; I (QD) and I' (dye) are the integrated emission peak areas at a given wavelength; A (QD) and A' (dye) are the absorption intensities at the same wavelength used for PL excitation; n (QD) and n' (dye) are the refractive indices of the solvents. According to the above-mentioned equation, we estimated the QY of Mn-doped ZnSe/ZnS quantum dots as 25%. TEM images were taken on a FEI TECNAI transmission electron microscope at an acceleration voltage of 200 kV. The suspensions of Mn-doped ZnSe/ZnS QDs were air-dried on a carbon-coated copper grid for TEM measurements. The FT-IR spectra were recorded on a VERTEX 70-FTIR spectrometer. Heavy metal ions were added into the probe soution and then the samples were separated from the solution followed by vacuum drying. The as-obtained powder samples were characterized by the FTIR spectrometer.

Addition of Heavy Metal ions in Colloidal Nanoparticle Solution. 5 μL of Hg^{2+} ion solution (20 nM) was added into 1 mL of the as-obtained solution containing colloidal nanoparticles. Experimental conditions for other heavy metal ions were the same as those for Hg^{2+} ions. Interference experiments were conducted through adding 5 μL of Hg^{2+} ions into the solutions in the presence of other heavy metal ions. The mixture was incubated for 30 seconds and then the fluorescence emission spectra were recorded at room temperature. Each spectrum was recorded repeatedly for at least three times. After the mercury ions completely reacted with functionalized QDs, the fluorescent intensity was stable, which is beneficial for taking accurate data. Therefore, fluorescent intensity of probe solution at 588 nm as a function of time was measured after adding mercury ions. By means of several measurements, 30 seconds as a response time is enough to obtain stable fluorescent data.

Detection of Real Samples. Drinking water was prepared as real analysis samples. The samples were filtered using 0.22 micrometer membrane to remove small solid particles followed by adding mercury ions. Different concentrations of mercury ion were prepared using these real samples as solvents for further use. The detection procedure for drinking water is the same as that mentioned above.

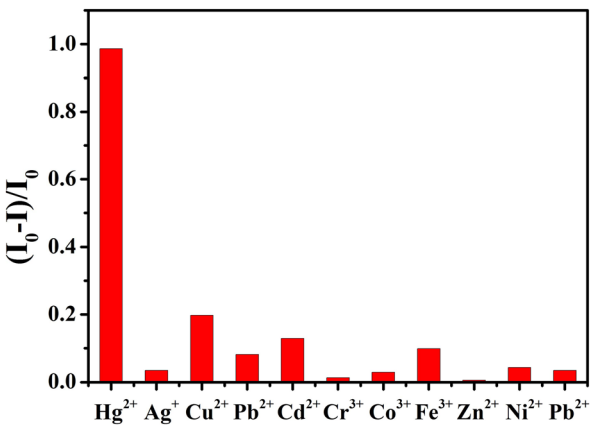

Figure 9 | The fluorescent response of MPA-coated Mn-ZnSe/ZnS (λ_{max} = 588 nm) in the presence of various heavy metal ions at 20 nM. The excitation wavelength was 400 nm.

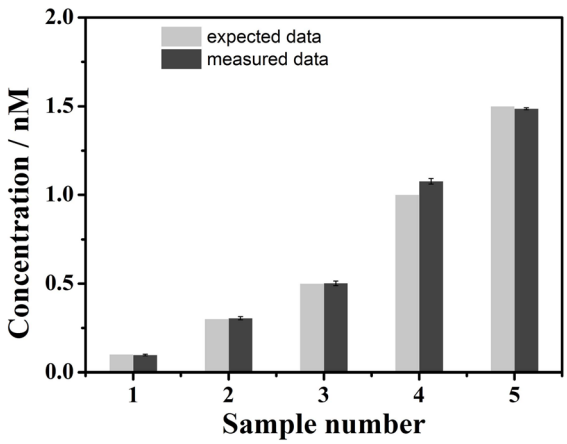

Figure 10 | Determination of Hg^{2+} ions in drinking water samples using the proposed method (dark gray column).

1. Campbell, L. M., Dixon, D. G. & Hecky, R. E. A review of mercury in Lake Victoria, East Africa: Implications for human and ecosystem health. *J. Toxicol. Env. Heal. B* **6**, 325–356 (2003).
2. Robinson, S. A., Lajeunesse, M. J. & Forbes, M. R. Sex Differences in Mercury Contamination of Birds: Testing Multiple Hypotheses with Meta-Analysis. *Environ. Sci. Technol.* **46**, 7094–7101 (2012).
3. Hopkins, B. C., Willson, J. D. & Hopkins, W. A. Mercury Exposure is Associated with Negative Effects on Turtle Reproduction. *Environ. Sci. Technol.* **47**, 2416–2422 (2013).
4. Huang, X. *et al*. Mercury Emissions from Biomass Burning in China. *Environ. Sci. Technol.* **45**, 9442–9448 (2011).
5. Neff, M. R. *et al*. Long-term changes in fish mercury levels in the historically impacted English-Wabigoon River system (Canada). *J. Environ. Monitor.* **14**, 2327–2337 (2012).
6. Smith, A. *et al*. Mercury Contamination of the Fish Community of a Semi-Arid and Arid River System: Spatial Variation and the Influence of Environmental Gradients. *Environ. Toxicol. Chem.* **29**, 1762–1772 (2010).
7. Liu, Z. F. *et al*. Dielectric barrier discharge-plasma induced vaporization and its application to the determination of mercury by atomic fluorescence spectrometry. *Analyst* **136**, 4539–4544 (2011).
8. Rodrigues, J. L. *et al*. Determination of total and inorganic mercury in whole blood by cold vapor inductively coupled plasma mass spectrometry (CV ICP-MS) with alkaline sample preparation. *J. Anal. Atom. Spectrom.* **24**, 1414–1420 (2009).
9. Li, M., Wang, Q. Y., Shi, X. D., Hornak, L. A. & Wu, N. Q. Detection of Mercury(II) by Quantum Dot/DNA/Gold Nanoparticle Ensemble Based Nanosensor Via Nanometal Surface Energy Transfer. *Anal. Chem.* **83**, 7061–7065 (2011).
10. Huang, C. C., Yang, Z., Lee, K. H. & Chang, H. T. Synthesis of highly fluorescent gold nanoparticles for sensing Mercury(II). *Angew. Chem. Int. Edit.* **46**, 6824–6828 (2007).
11. Deng, L., Zhou, Z. X., Li, J., Li, T. & Dong, S. J. Fluorescent silver nanoclusters in hybridized DNA duplexes for the turn-on detection of Hg^{2+} ions. *Chem. Commun.* **47**, 11065–11067 (2011).
12. Cho, Y., Lee, S. S. & Jung, J. H. Recyclable fluorimetric and colorimetric mercury-specific sensor using porphyrin-functionalized Au@SiO_2 core/shell nanoparticles *Analyst* **135**, 1551–1555 (2010).
13. Kalluri, J. R. *et al*. Use of Gold Nanoparticles in a Simple Colorimetric and Ultrasensitive Dynamic Light Scattering Assay: Selective Detection of Arsenic in Groundwater. *Angew. Chem. Int. Edit.* **48**, 9668–9671 (2009).
14. Chan, W. C. W. & Nie, S. M. Quantum dot bioconjugates for ultrasensitive nonisotopic detection. *Science* **281**, 2016–2018 (1998).
15. Yu, J. H. *et al*. High-resolution three-photon biomedical imaging using doped ZnS nanocrystals. *Nat. Mater.* **12**, 359–366 (2013).
16. Paramanik, B., Bhattacharyya, S. & Patra, A. Detection of Hg^{2+} and F^- Ions by Using Fluorescence Switching of Quantum Dots in an Au-Cluster-CdTe QD Nanocomposite. *Chem. Eur. J.* **19**, 5980–5987 (2013).
17. Gaponik, N., Talapin, D. V., Rogach, A. L., Eychmuller, A. & Weller, H. Efficient phase transfer of luminescent thiol-capped nanocrystals: From water to nonpolar organic solvents. *Nano Lett.* **2**, 803–806 (2002).
18. Lesnyak, V., Gaponik, N. & Eychmuller, A. Colloidal semiconductor nanocrystals: the aqueous approach. *Chem. Soc. Rev.* **42**, 2905–2929 (2013).
19. Gaponik, N. Assemblies of thiol capped nanocrystals as building blocks for use in nanotechnology. *J. Mater. Chem.* **20**, 5174–5181 (2010).
20. Zhang, Y. J., Schnoes, A. M. & Clapp, A. R. Stable water-soluble quantum dots capped by poly(ethylene glycol) modified dithiocarbamate. *ACS Appl. Mater. Inter.* **2**, 3384–3395 (2010).
21. Han, B. Y., Yuan, J. P. & Wang, E. K. Sensitive and selective sensor for biothiols in the cell based on the recovered fluorescence of the CdTe quantum dots-Hg(II) system. *Anal. Chem.* **81**, 5569–5573 (2009).
22. Xia, Y. S. & Zhu, C. Q. Use of surface-modified CdTe quantum dots as fluorescent probes in sensing mercury (II). *Talanta* **75**, 215–221 (2008).
23. Zhang, X. L., Xiao, Y. & Qian, X. H. A Ratiometric Fluorescent Probe Based on FRET for Imaging Hg^{2+} Ions in Living Cells. *Angew. Chem. Int. Edit.* **47**, 8025–8029 (2008).
24. Han, J. S. *et al*. Fabrication of CdTe nanoparticles-based superparticles for an improved detection of Cu^{2+} and Ag^{+}. *J. Mater. Chem.* **22**, 2679–2686 (2012).
25. Zeng, R. S., Rutherford, M., Xie, R. G., Zou, B. S. & Peng, X. G. Synthesis of Highly Emissive Mn Doped ZnSe Nanocrystals without Pyrophoric Reagents. *Chem. Mater.* **22**, 2107–2113 (2010).
26. Pradhan, N. & Peng, X. G. Efficient and color-tunable Mn doped ZnSe nanocrystal emitters: Control of optical performance via greener synthetic chemistry. *J. Am. Chem. Soc.* **129**, 3339–3347 (2007).
27. Acharya, S., Sarma, D. D., Jana, N. R. & Pradhan, N. An Alternate Route to High-Quality ZnSe and Mn Doped ZnSe Nanocrystals. *J. Phys. Chem. Lett.* **1**, 485–488 (2010).
28. Wang, C., Gao, X., Ma, Q. & Su, X. G. Aqueous synthesis of mercaptopropionic acid capped Mn^{2+} doped ZnSe quantum dots. *J. Mater. Chem.* **19**, 7016–7022 (2009).
29. Graf, C. *et al*. Magnetic and Structural Investigation of ZnSe Semiconductor Nanoparticles Doped With Isolated and Core-Concentrated Mn^{2+} Ions. *Adv. Funct. Mater.* **19**, 2501–2510 (2009).
30. Hofmann, A., Graf, C., Boeglin, C. & Ruhl, E. Magnetic and structural investigation of Mn^{2+} - doped ZnSe semiconductor nanoparticles. *Chemphyschem* **8**, 2008–2012 (2007).
31. Hines, M. A. & Guyot-Sionnest, P. Synthesis and characterization of strongly luminescing ZnS Capped CdSe nanocrystals. *J. Phys. Chem.* **100**, 468–471 (1996).
32. Ke, J., Li, X. Y., Shi, Y., Zhao, Q. D. & Jiang, X. C. A facile and highly sensitive probe for Hg(II) based on metal-induced aggregation of ZnSe/ZnS quantum dots. *Nanoscale* **4**, 4996–5001 (2012).
33. Pradhan, N., Goorskey, D., Thessing, J. & Peng, X. G. An alternative of CdSe nanocrystal emitters: Pure and tunable impurity emissions in ZnSe nanocrystals. *J. Am. Chem. Soc.* **127**, 17586–17587 (2005).
34. Liu, J. B. *et al*. Aggregation Control of Quantum Dots through Ion-Mediated Hydrogen Bonding Shielding. *ACS Nano* **6**, 4973–4983 (2012).
35. Grasso, D., Subramaniam, K., Butkus, M., Strevett, K. & Bergendahl, J. A review of non-DLVO interactions in environmental colloidal systems. *Rev. Environ. Sci. Biotechnol.* **1**, 17–38 (2002).
36. Bian, S. W., Mudunkotuwa, I. A., Rupasinghe, T. & Grassian, V. H. Aggregation and Dissolution of 4 nm ZnO Nanoparticles in Aqueous Environments: Influence of pH, Ionic Strength, Size, and Adsorption of Humic Acid. *Langmuir* **27**, 6059–6068 (2011).
37. Zhang, H. *et al*. Fine-Tuning the Surface Functionality of Aqueous Luminescent Nanocrystals through Surfactant Bilayer Modification. *Langmuir* **24**, 12730–12733 (2008).
38. Zhang, H. *et al*. Directing the Growth of Semiconductor Nanocrystals in Aqueous Solution: Role of Electrostatics. *Chemphyschem* **9**, 1309–1316 (2008).
39. Li, Y. S. *et al*. Enhanced photocatalytic activities of TiO_2 nanocomposites doped with water-soluble mercapto-capped CdTe quantum dots. *Appl. Catal. B-Environ.* **101**, 118–129 (2010).
40. Fang, Z., Li, Y., Zhang, H., Zhong, X. H. & Zhu, L. Y. Facile Synthesis of Highly Luminescent UV-Blue-Emitting ZnSe/ZnS Core/Shell Nanocrystals in Aqueous Media. *J. Phys. Chem. C* **113**, 14145–14150 (2009).
41. Duan, J. L., Song, L. X. & Zhan, J. H. One-Pot Synthesis of Highly Luminescent CdTe Quantum Dots by Microwave Irradiation Reduction and Their Hg^{2+} Sensitive Properties. *Nano Res.* **2**, 61–68 (2009).
42. Yao, J. J., Schachermeyer, S., Yin, Y. D. & Zhong, W. W. Cation Exchange in ZnSe Nanocrystals for Signal Amplification in Bioassays. *Anal. Chem.* **83**, 402–408 (2011).
43. Ali, S. R. *et al*. A nonoxidative sensor based on a self-doped polyaniline/carbon nanotube composite for sensitive and selective detection of the neurotransmitter dopamine. *Anal. Chem.* **79**, 2583–2587 (2007).
44. Wu, P. *et al*. Semiconductor quantum dots-based metal ion probes. *Nanoscale* **6**, 43–64 (2014).
45. Li, J. J. *et al*. Large-Scale Synthesis of Nearly Monodisperse CdSe/CdS Core/Shell Nanocrystals Using Air-Stable Reagents via Successive Ion Layer Adsorption and Reaction. *J. Am. Chem. Soc.* **125**, 12567–12575 (2003).

Acknowledgments

This work was supported financially by the National Nature Science Foundation of China (21377015, 21207015, N_HKUST646/10), the Major State Basic Research Development Program of China (973 Program) (No. 2011CB936002) and the Key Laboratory of Industrial Ecology and Environmental Engineering, China Ministry of Education. J.H.C. acknowledges financial support from the U.S. National Science Foundation (IIP-1128158).

Author contributions

X.Y.L. and J.K. conceived the experiments. J.K. prepared the samples and wrote the manuscript. X.Y.L., Q.D.Z., Y.H. and J.H.C. contributed to the analysis and discussion of the results. All authors reviewed the manuscript.

Additional information

Supplementary information accompanies this paper at http://www.nature.com/scientificreports

Competing financial interests: The authors declare no competing financial interests.

How to cite this article: Ke, J., Li, X., Zhao, Q., Hou, Y. & Chen, J. Ultrasensitive Quantum Dot Fluorescence quenching Assay for Selective Detection of Mercury Ions in Drinking Water. *Sci. Rep.* **4**, 5624; DOI:10.1038/srep05624 (2014).